HEFAT2007
5th International Conference on Heat Transfer, Fluid Mechanics and Thermodynamics
Sun City, South Africa
Paper number: HF1

ANALYSIS OF SUPERSONIC EJECTOR OPERATION: EXPERIMENTAL VALIDATION AND TWO-PHASE ASPECTS

François Henry, Sébastien Leclaire, Amel Hemidi, Jean-Marie Seynhaeve, and Yann Bartosiewicz [a]
[a] Corresponding author
Université catholique de Louvain UCL, Faculty of Applied Sciences, Mechanical Engineering Department, TERM Division, Place du Levant 2, B-1348, Louvain-la-Neuve, Belgium.
Email: yann.bartosiewicz@term.ucl.ac.be, Tel: +32 10 47 22 06, Fax: +32 10 45 26 92

ABSTRACT

This paper deals with comparisons between CFD and experiments for a supersonic ejector. We present good results in terms of entrainment prediction compared to home-made experimental data for an air ejector. Over the whole range of operating conditions, the deviation is below 10% for the $k-\varepsilon$ model. In addition, a first attempt to tackle two-phase aspects was also performed experimentally and by simulations.

INTRODUCTION

Supersonic ejectors are simple mechanical devices (Figure 1), which can be used to pump and compress a given flow without any moving parts. By an entrainment-induced effect, the secondary stream is drawn into the ejector and eventually compressed to the back pressure. For a detailed flow physics analysis in ejectors, readers should refer to [1–3]. One of the most promising application is the steam jet refrigeration as an environment-friendly technology in a response to the problem of global warming (GHG emissions) or ozone depletion. In this paper, the targeted application is the use of supersonic ejectors in air conditioning [4,5] and refrigeration [6,7] areas to realize thermal compression activated by low-grade heat release or a renewable source. A good overview of the different applications in this field may be found in the review articles of Sun and Eames [8], Chunnanond and Aphornratana [7], and more recently Riffat et al. [9]. However, the development of such systems at industrial scales is limited due to their efficiency and stability at off-design conditions raising the problem of their control. From the CFD point of view, even though the number of studies is still growing and highlight the potential of this tool in the understanding, design and forecast ejector operations, a lot of questions still remain. Indeed, most of the studies [10–12] assume, without any comparison, that the standard $k-\varepsilon$ model is able to give good results although some authors [2, 3, 13] highlight the large sensitivity of the chosen turbulence approach depending on the ejector operations. In addition, the authors [2] raised the problem of a rigourous CFD-experiment integration in so far as CFD conditions often does not match experiment conditions in terms of boundary conditions or geometric design. The last comparative study [11] showed that CFD prediction could satisfactorily predict the on-design operation and the critical point, but failed in the prediction of the off-design mode since errors could reach 40%-50%. In addition, real gas properties [3, 10] and the two-phase nature of the flow that changes its critical properties, are some questions very scarcely raised in literature. The only study that attempts to tackle the two-phase aspect, but for other reasons, is that of Al-Ansary et al. [13, 14] who introduced fine droplets into the primary stream and noted some performance improvements for off-design conditions. However, the relative influence of tested parameter was not clear and first CFD tests were enable to predict such behavior but were contradictory. The study started in our team will be devoted to ejector air conditioning with a special focus on the critical two phase-flow aspects with a CFD-experiment integration approach.

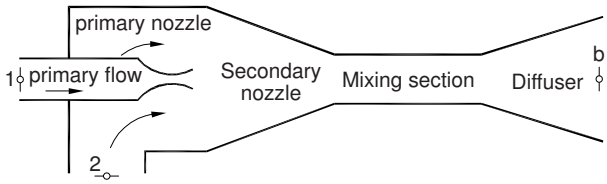

Figure 1: A typical ejector geometry

MODELING APPROACH

GOVERNING EQUATIONS

The flow in the air-ejector is governed by the ideal gas compressible steady-state axisymmetric form of the fluid flow conservation equations. For variable density flows, the Favre averaged Navier-Stokes (FANS) equations are more suitable and will

be used in this work. The total energy equation including viscous dissipation is also included and coupled to the set with the perfect gas law. The thermodynamics and transport properties for air are held constant; their influence was not found to be significant during previous tests. In this paper, water droplets are injected into the primary flow, as proposed and performed experimentally by Al- Ansary and Jeter [14]. These water droplets are considered spherical and are modelled as a discrete second phase in a Lagrangian frame. In order to take into account the coupling between the continuous and the dispersed phase, a source term is added to the momentum (F_p). Thus for single phase computations, $F_p = 0$.
The trajectories are predicted by integrating the force balance on the particles:

$$\frac{du_p}{dt} = F_D(u - u_p) \tag{1}$$

where F_D stands for the drag force coefficient per unit particle mass and it is written:

$$F_D = \frac{18\mu}{\rho_p {d_p}^2}\frac{C_D R_e}{24} \tag{2}$$

For the continuous phase the drag source term then becomes in its discretized manner:

$$F_p = F_D(u_p - u)\dot{m}_p \Delta t \tag{3}$$

This set of equations is solved by a control volume approach in the CFD commercial package FLUENT 6.2. Although the steady state is desired, the unsteady term is conserved since from a numerical point of view, governing equations are solved with a time marching technique. This allows to keep equations parabolic-hyperbolic for every Mach number. The system is also time-preconditioned in order to overcome the problem of numerical stiffness at low-mach numbers. The convection term is discretized with a flux splitting method in order to capture shock accurately (second order upwind), while the diffusive term uses a central difference discretization. The coupled system is then solved by a block Gauss-Seidel method with an algebraic multigrid acceleration algorithm. Concerning turbulence modeling, Bartosiewicz et al. [2,3] showed from preliminary tests that local behavior in terms of local flow structures is strongly dependant of the turbulence model. However it was difficult to conclude because of possible mismatches between numerical and experimental boundary conditions. For conciseness reasons, the reader is referred to references [2, 3] for more details about the features and performance of this turbulence models or other algorithm features.

NUMERICAL ACCURACY AND CONVERGENCE

The criterion for assessing convergence was based on the root mean square of the equation residues expressed by:

$$R(\zeta) = \left[\sum_{i=1}^{N}\left(\frac{\partial \zeta}{\partial t}\right)_i^2\right]^{1/2} \tag{4}$$

where N is the number of grid points and ζ is the considered variable (mass, energy, momentum, etc.). Generally, computation are stopped when residues fall below $1 * 10^{-6}$ and remain stable. In addition, at convergence the mass imbalance is checked and should be:

$$\left|\frac{\sum \dot{m}_{in} - \sum \dot{m}_{out}}{\sum \dot{m}_{in}}\right| \tag{5}$$

The time step is setup by a Courant-Friedrichs-Lewy (CFL) conditions. At the beginning of calculations it is set to 0.5, because the solution is highly non-linear, and it is increased up to 5 at the end due the implicit time discretization. Moreover, before to proceed deep analysis, a grid convergence study was performed to ensure overall mesh independent results. For instance the calculated deviations for the primary and secondary mass flow rate were respectively 0.44% and 1.16% for the two different meshes (25820 cells and 88566 cells).

Finally, mesh 1 (25820 cells) (Figure 2) was considered sufficient to give satisfactory results in term of entrainment ratio. This mesh is refined from the primary nozzle lips along the shear layer and also close to walls. In most of the case the overall value for the wall coordinate is $y^+ \approx 1$.

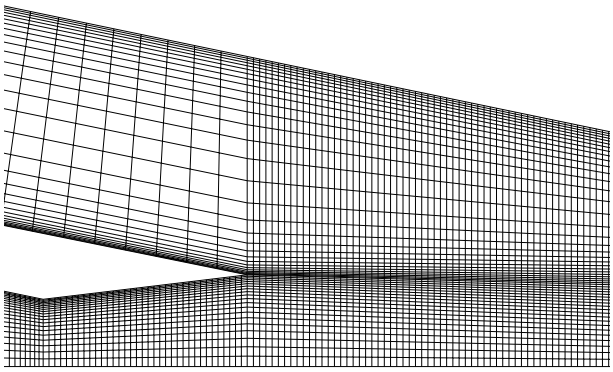

Figure 2: A part of the computational mesh

EXPERIMENTAL APPARATUS

DESCRIPTION OF THE EXPERIMENTAL SET-UP

A sketch of the experimental apparatus is given Figure 3.

The experimental apparatus is equipped with the following elements:

- An upstream vessel of 5 m^3 filled with compressed air at about 7 bar.
- A pressure reducer.
- The primary pipe equipped with a flow measuring device.
- The ejector to be tested (Figure 4).
- The secondary pipe also equipped with a flow measuring device and connected to the atmosphere.
- The exhaust pipe equipped with manual adjustable valve.

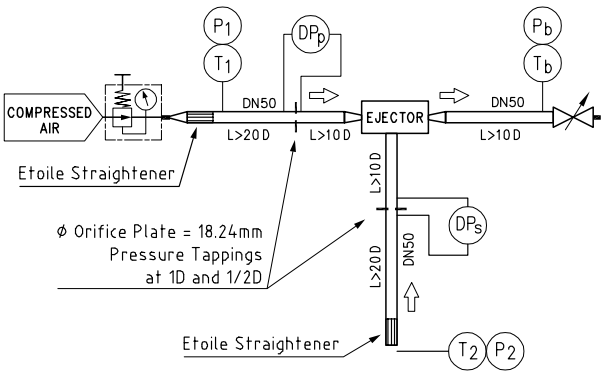

Figure 3: Sketch of the experimental set-up

The tests of the ejector were conducted at constant driving pressure in the primary pipe which can be finely controlled by the pressure reducer. Three different primary pressures P_1 were tested : 4 bar, 5 bar and 6 bar. For each of these pressures, the back-pressure at the exhaust pipe was controlled by the manual valve. The choice of the back-pressure was firstly dictated by the total back pressure obtained in the different simulations. The pressure in the secondary pipe was maintained at atmospheric pressure and measured to adjust CFD computation. As shown Figure 4, the secondary air stream is supplied through an annular entrance in order to ensure an axisymmetric flow pattern to match CFD conditions (axisymmetric solver).

Some tests have been performed with water droplets injection into the primary air stream. These droplets were produced by an ultrasonic atomizer (UCL patent 09900790) spray, courtesy provided by the compagny POLYSPRAY, and which is able to create a quasi monodispersed granulometric curve of droplets. The chosen atomizer provided droplets of 50 μm in diameter.

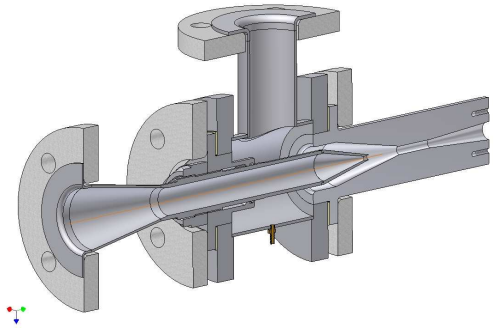

Figure 4: Sketch of the experimental set-up

DESCRIPTION OF THE INSTRUMENTATION

The pressures P_1 and P_b are measured by effective pressure transducers which have been previously calibrated with a manometric balance. The differential pressure transducers used in the flow measuring devices have been calibrated with a Betz manometer. These calibrations have been carried out just before the experimental campaign. The temperatures are measured by PT100 sensors of type A which ensure an uncertainty less than 0.1 $^{\circ}C$. The mass flow rate are determined from an orifice plate device equipped with 1D and 1/2 D pressure taps according to the ISO 5167 standard. The uncertainties on all the quantities (pressures, temperatures, mass flow rates, etc.) have been determined according to the Guide of Uncertainties on Measurements (GUM). These uncertainties have been reported in Figure 5.

EXPERIMENTAL RESULTS

The experimental results are shown Figure 5. In this Figure, we can clearly observe the typical characteristic of the ejector, i.e. a constant mass flow rate corresponding to choked flow conditions in the secondary nozzle, followed by a quasi linear and a relatively stiff decreasing of the secondary mass flow rate.

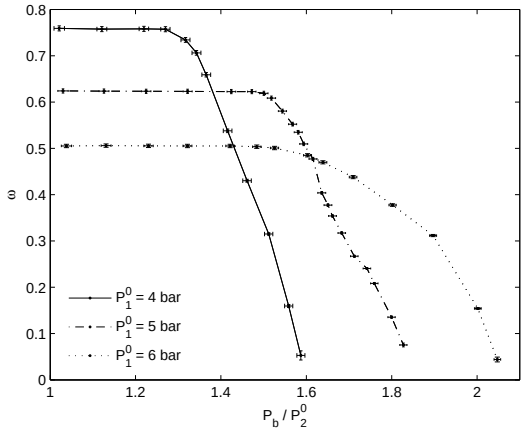

Figure 5: Ejector characteristics- Experimental results

RESULTS AND DISCUSSIONS

CFD VALIDATION: SINGLE-PHASE FLOW

For this validation part, the main dimensions of the ejector are depicted figure 6. The total length of the ejector is 22.5mm for 25820 cells. Originally, this geometry was designed for a real refrigeration cycle using butane as the working fluid and follows the ESDU and ASHRAE prescriptions. In this paper, this ejector is tested with air in order to assess CFD models in terms of operation features for a broad range of conditions. Therefore, the geometry characteristics such as the distance between the primary nozzle and the inlet of the mixing chamber is kept constant to $\Delta L = 3D^*$, $d^* = 3.3mm$, $d = 4.5mm$, $D^* = 7.6mm$. As our interest is focus on refrigeration applications, it is relevant to sweep the different ejector operation modes by changing the back-pressure P_b for constant primary and secondary pressures P_1 and P_2. Indeed, for this case, the back-pressure would be that of the condenser which is strongly dependent of the ambient conditions. The secondary pressure is roughly constant during a

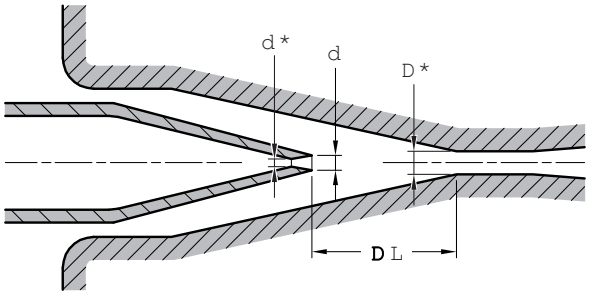

Figure 6: Main ejector dimensions

test series and equal the atmospheric pressure; it is measured for each tested conditions and incorporated in the CFD model. In addition, both the primary and secondary pressures measured are static pressures; their values are incorporated in the CFD model as total pressures in so far as the respective velocities have been calculated to few meters per second providing static and total pressures equal. Consistently with measurements, the two cases $P_1^0 = 4bar$ and $P_1^0 = 5bar$ have been carried out. For those cases, the turbulence intensities and the viscosity ratios at inlets were prescribed to $I_{\%} = 0.05$ and $\mu_t = 2 * \mu_l$ according to a fully turbulent pipe flow. All the walls are assumed adiabatic. Figures 7 and 8 illustrate the results in comparison with experimental data. First of all, the general shape of the ejector characteristics curves is well reproduced by CFD, as noted by some authors [11,13]: as the back-pressure is decreased down to a critical pressure, the entrainment ratio $\omega = \dot{m}_2/\dot{m}_1$ increases up to reach a plateau where the secondary mass flow rate and thus ω remains constant. At this pressure the ejector is said choked and works at on-design conditions. For a higher P_b it operates at off-design conditions. The overall results show that CFD tends to slightly overestimate the maximum entrainment rate, which is in contradiction to Sriveerakul and al. [11] observations. In addition, the different be-

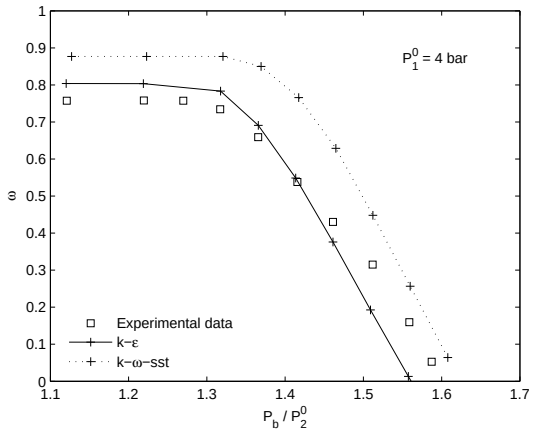

Figure 7: Comparison CFD-experiments for $P_1^0 = 4b$

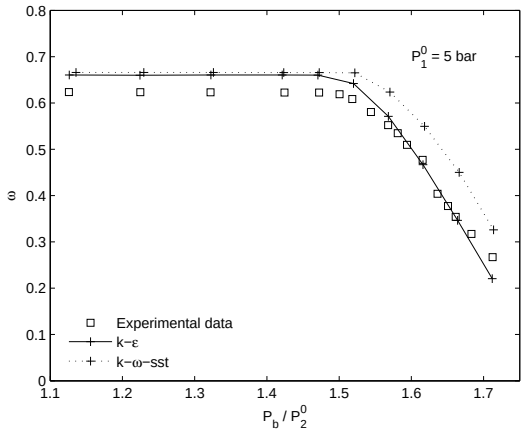

Figure 8: Comparison CFD-experiments for $P_1^0 = 5b$

haviors between $k-\varepsilon$ and $k-\omega-sst$ turbulence models depend on the primary pressure. Indeed, figure 7 illustrates a significant offset toward higher ω values and over the whole range of tested conditions for $k-\omega-sst$ results concerning $P_1^0 = 4bar$. However, for $P_1^0 = 5bar$ (Fig. 8), $k-\varepsilon$ and $k-\omega-sst$ give the same entrainment ratio at on-design conditions, discrepancies taking place beyond the critical point and at off-design conditions. Ongoing simulations at higher and lower pressures seem to confirm the trend of a better agreement as the primary pressure is increased. However, this behavior needs further analysis and explanations since even though both models give the same ω for $P_1^0 = 5bar$, local flow features (not shown here) seem very different. The error distributions compared to experimental points

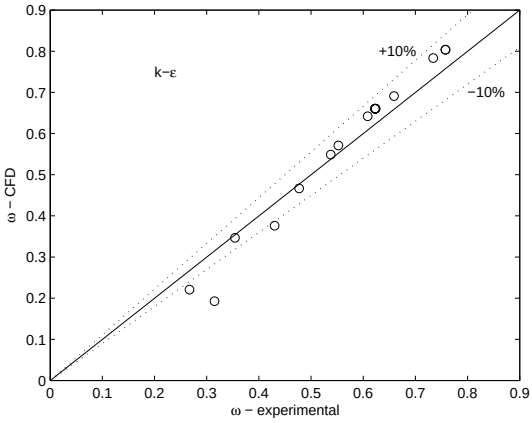

Figure 9: Errors distribution for $k-\varepsilon$

for each model and for the whole range of tested conditions (on-design, off-design, both primary pressures) are presented figures 9 and 10. For the $k-\varepsilon$ the quantitative agreement is very good either for on-design or off-design conditions, contrary to [11] where 40%-50% deviations could be observed in the off-design

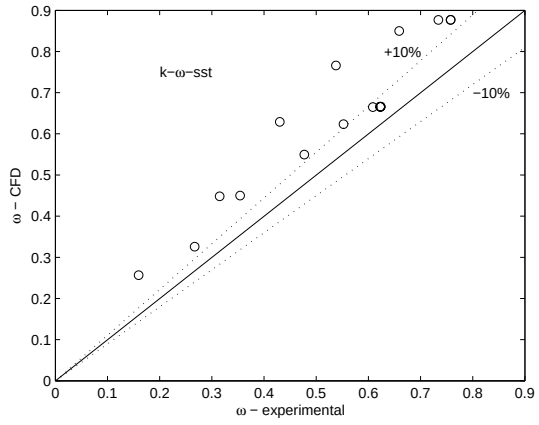

Figure 10: Errors distribution for $k-\omega-sst$

region. In the present results, all points except in the deep off-design area, represent a deviation below 10%. However, results are generally better for the case $P_1^0 = 5bar$ (Figs. 7 and 8).

Even though most of the results obtained with the $k-\omega-sst$ model are largely outside a deviation of 10% (Fig. 10), it is noted that for deeper off-design conditions, close to the secondary flow reversal ($\dot{m}_2 < 0$), the agreement with the $k-\omega-sst$ tends to improve. This comes from that a slope change can be observed at some points in experimental data (Figs .7 and 8) and this behavior seems systematically observed. Furthers tests will have to be achieved to know whether this feature is due to difficult measurements at low entrainment because high sensitivity to boundary conditions, or it is due to a physical flow characteristic. However, the current test stand does not allow to measure negative secondary flow rate, and measurement become extremely sensitive to back-pressure at higher compression rate.

TWO-PHASE FLOW ASPECTS

As mentioned in introduction, the only study about the effect of two-phase flow on the ejector operation is that of Al-Ansary et al. [14]. In this experiment, fine water droplets($17\mu m$ according to the manufacturer) are injected at the primary inlet owing to a two-phase atomizer. In their paper, authors [14] reported a significant increase of the entrainment ratio when water droplets are injected, and this effect was only observed at off-design conditions and for low primary pressure (below 2.5 bar). Their increase reached 98% in the best case. However some inherent limitations were not discussed such as wall effects which can prevent all the water injected to cross the ejector because of water accumulation, possible vaporization-condensation effect. In addition, the definition of the two-phase entrainment ratio did not take into account the water mass flow rate and the additional compressed air supplied to the atomizer, which is able to moderate the improvement. In this study, water droplets are injected with an ultra-sonic atomizer which does not need any additional air to atomize water; this is achieved through a vibrating device at a specific resonance frequency. In addition, a purge system was set up to recover and measure the amount of water that did not cross the ejector because of upstream accumulations. This device allowed to measure the average water mass flow rate during an experiment : for instance, it was found that 22.3% of water was lost at a total water flow rate of $0.5l.h^{-1}$. For those tests, the two previous ejector characteristics, for $P_1^0 = 4bar$ and $P_1^0 = 5bar$, have been remeasured and compared according to the type of flow: results are presented Figure 11. For both conditions, the average water mass fraction injected at the primary inlet is roughly the same and about 1%, which is much less than that claimed by Al-Ansary et al. [14] (about 10% maximum). Figure 11 clearly illustrates that the presence of water droplets has no significant effect at on-design operation. But this effect becomes significant at critical point and beyond at off-design operation. It can be observed that the critical point is slightly moved toward higher backpressures, providing a potential extent of the on-design operation. At off-design operation, the maximum difference at low entrainment rate may even reach 115%. Those results are very interesting because in real situation liquid droplets could come from an upstream condensation in the primary steam line or in the nozzle.

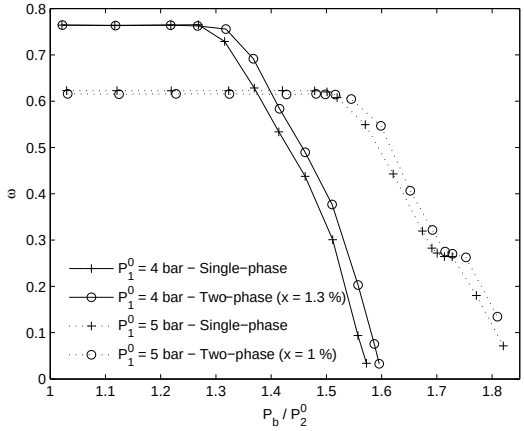

Figure 11: Entrainment ratio: single-phase vs. two-phase flow

In order to understand this two-phase behavior, CFD simulations were performed with a simple discrete phase model for inert water droplets. The chosen condition was the case where $P_1^0 = 4bar$ and $P_b = 1.45bar$. For that condition, the experimental improvement in terms of entrainment ratio was about 12%. Results are summurized table 1. For the given experimental conditions, the model predicts an entrainment rate of $\omega = 0.336$ compared to $\omega = 0.379$ for single phase, which represents a decrease of 11.5% : this is totally in contradiction with experiments. This kind of results was mentioned in the thesis of Al-Ansary [13]. In addition, when the diameter of water droplets is decreased, keeping constant mass fraction, simulations predict a more important decrease, fairly zero for $d_d = 5\mu m$. This result is in contradiction to what was observed by Al-Ansary [13] who claimed that finer droplets could improve entrainment by decreasing momentum mismatch between primary and secondary streams. Moreover,

when the mass flow rate was increased to values close to those of Al-Ansary [14], the ejector operation tuned out into malfunction mode since reversal flow occurred at secondary outlet. It is believed that inert discrete phase model is inappropriate and two-phase aspects deserve further investigations.

Table 1: CFD entrainment ratios for different particle diameters and mass fractions

d_d (μm) / x (%)	150	100	50	15	5
1.33	0.350	0.343	0.336	0.29	0.08
15	-	-	< 0	-	< 0

CONCLUDING REMARKS

In this paper an integrated and a balanced CFD-experiment study was presented for a supersonic ejector working with air. Using air to test and validate thermofluid models may be useful because experimental set is very simple and a wide range of measurement may be achieved compared to a closed refrigerant system. In addition, we believe that CFD could scale-up such devices in order to extrapolate results to other fluids. In this work, good validation results have been obtained for a wide range of operating condition and were generally in a better qualitative agreement that those found in literature, especially for the off-design operation. It is believed such good results may be mostly attributed to the special focus of setting up a test bench and boundary conditions measurement as close as possible of those of the CFD. In addition, it has been clearly demonstrated that the presence of liquid droplets in the primary stream, which could physically come from condensation, is not necessarily harmful to the ejector operation but on contrary may significantly improve its off-design operation. However, a large range of two-phase situation needs to be experienced and a consistent compressible two-phase CFD model needs to be set up. In this sense, we believed that such a model should take into account vaporization-condensation, nucleation and the two-phase definition of sound speed in order to correctly model these two-phase critical flows. In addition, flow visualization would help to understand some phenomena (wall effect, etc.)

ACKNOWLEDGEMENT

Author wish to acknowledge the General Directorate for Technology, Research and Energy (D.G.T.R.E.) of the Ministry for Belgium's Walloon Region to financially support the PROFESSI project. Authors would also to thank all the technical staff of the TERM division for its help in the set-up of the experimental stand, and the company POLYSPRAY (info@polyspray.be) for providing and adjusting the ultra-sonic atomizer.

REFERENCES

[1] K. Matsuo, Y. Miyazato, and H. D. Kim. Shock train and pseudo-shock phenomena in internal gas flows. *Progress in Aerospaces*, 35:33–100, 1999.

[2] Y. Bartosiewicz, Z. Aidoun, P. Desevaux, and Y. Mercadier. Numerical and experimental investigations on supersonic ejectors. *International Journal of Heat and Fluid Flow*, 26:56–70, 2005.

[3] Y. Bartosiewicz, Z. Aidoun, and Y. Mercadier. Numerical assessment of ejector operation for refrigeration applications based on cfd. *Applied Thermal Engineering*, 26(5-6):604–612, 2006.

[4] S. B. Riffat, G. Gan, and S. Smith. Computational fluid dynamics applied to ejector heat pumps. *Applied Thermal Engineering*, 16(4):291–297, 1996.

[5] S. B. Riffat and P. Everitt. Experimental and cfd modelling of an ejector system for vehicle air conditioning. *Journal of the Institute of Energy*, 72:41–47, 1999.

[6] B. J. Huang, V. A. Petrenko, J. M. Chang, C. P. Lin, and S. S. Hu. A combined cycle refrigeration system using ejector-cooling as the bottom cycle. *International Journal of Refrigeration*, 24(5):391–399, 2001.

[7] K. Chunnanond and S. Aphornratana. Ejectors: Applications in refrigeration technology. *Renewable & Sustainable Energy Reviews*, 8:129–155, 2004.

[8] D. W. Sun and I. W. Eames. Recent development in the design theories and applications of ejectors - a review. *Journal of the Institute of Energy*, 68:65–79, 1995.

[9] S. B. Riffat, L. Jiangang, and G. Gan. Recent development in ejector technology - a review. *International Journal of Ambient Energy*, 26(1):13–26, 2005.

[10] E. Rusly, L. Aye, W. W. S. Charters, and A. Ooi. Cfd analysis of ejector in a combined ejector cooling system. *International Journal of Refrigeration*, 28:1092–1101, 2005.

[11] T. Sriveerakul, S. Aphornratana, and K. Chunnanond. Performance prediction of steam ejector using computational fluid dynamics: Part 1. validation of the cfd results. *International Journal of Termal Sciences*, in press.

[12] T. Sriveerakul, S. Aphornratana, and K. Chunnanond. Performance prediction of steam ejector using computational fluid dynamics: Part 2. flow structure of a steam ejector influenced by operating pressures and geometries.

[13] H. A. M. Al-Ansary. *Study of Single-phase and Two-phase Ejectors*. PhD thesis, Georgia Institute of Technology, 2004.

[14] H. A. M. Al-Ansary and S. M. Jeter. Numerical and experimental analysis of single-phase and two-phase flow in ejectors. *HVAC & R Research*, 10(4):521–538, 2004.